Hindawi
Advances in Materials Science and Engineering
Volume 2018, Article ID 2314794, 5 pages
https://doi.org/10.1155/2018/2314794

Research Article

One-Step Synthesis of Conductive BNC/PPy·$CuCl_2$ Hybrid Flexible Nanocomposites by *In Situ* Polymerization

Daliana Müller,[1,2] Bruno N. Wesling,[2] Gabriella M.V. Dias,[1,2] Joseane C. Bernardes,[1,2] Luismar M. Porto,[4] Carlos R. Rambo ,[1,2,3] and Dachamir Hotza [1,4]

[1]*Graduate Program of Materials Science and Engineering (PGMAT), Federal University of Santa Catarina (UFSC), 88040-900 Florianópolis, Brazil*
[2]*Laboratory of Electrical Materials (LAMATE), Federal University of Santa Catarina (UFSC), 88040-900 Florianópolis, Brazil*
[3]*Department of Electrical and Electronic Engineering (EEL), Federal University of Santa Catarina (UFSC), 88040-900 Florianópolis, Brazil*
[4]*Department of Chemical and Food Engineering (EQA), Federal University of Santa Catarina (UFSC), 88040-900 Florianópolis, Brazil*

Correspondence should be addressed to Carlos R. Rambo; carlos.rambo@ufsc.br

Received 30 May 2018; Revised 23 August 2018; Accepted 29 August 2018; Published 23 September 2018

Academic Editor: Zhiping Luo

This work reports the one-step synthesis of bacterial nanocellulose (BNC) incorporated with polypyrrole (PPy) by chemical *in situ* polymerization of pyrrole (Py) using $CuCl_2 \cdot 2H_2O$ as both oxidant agent and functional component, varying the concentration and molar ratio. Electrical, morphological, and physical-chemical properties of these nanocomposites were investigated. The results revealed that with the increase of Py concentration and molar ratio, the nanocomposites presented traces of copper chloride and copper oxide as shown by Raman and XRD analysis. The quality of bacterial cellulose nanofibers coating by the polymer and the electrical conductivity of the nanocomposites was directly affected by those variables. The combination of the conducting polymer with the oxidant agent offers possibilities for different applications such as electronic devices and sensors.

1. Introduction

Conducting polymers can be employed as active, functional components in flexible nanocomposites [1–3]. The interest in research on polymeric and hybrid nanocomposites containing both conductive polymers and oxide materials has attracted the attention of many research groups in recent years [1, 2]. Such class of nanocomposites shows great potential in various applications like sensors and other electronic devices, as they combine electrical, optical, and magnetic properties in one material [4–6].

Among the substrates for flexible electronics, bacterial nanocellulose (BNC) has been extensively applied in the synthesis of polymeric and hybrid nanocomposites mainly due to its low-cost and controllable synthesis process [7, 8]. Several studies have been performed in the polymerization of conductive polymers onto bacterial nanocellulose membranes for various applications such as sensors [9], electronic devices, and biomedical devices [10, 11].

The oxidative chemical polymerization in aqueous media of conducting polymers, such as polypyrrole and polyaniline, is widely used as a preparation method, because of the simplicity of the reaction [12, 13]. The electrical conductivity and other properties of these polymers depend on the preparation conditions. Fe (III) salts and ammonium persulfate are the most common oxidants used for polymerization of conductive polymers. Because of their potential of oxidation, other oxidants have been reported in the literature, such as sulfate of cerium IV [14], potassium dichromate [15], vanadium chloride [16], and copper (II) salts [17]. It is known that the use of different oxidizing agents tends to alter the electrical and morphological properties of conducting polymers [18]. However, studies on the use of different oxidants and their functionality in such composites are scarce, since they are usually removed, leaving only the compositional polymers.

This work reports the synthesis and characterization of flexible BNC/PPy·$CuCl_2$ nanocomposites in a single step through *in situ* oxidative polymerization with copper chloride dehydrate as both oxidant agent and conducting component in the nanocomposites. Structural and electrical properties were evaluated and related to the monomer concentration and the oxidant agent : monomer molar ratio.

2. Materials and Methods

2.1. Materials. Copper chloride dehydrate ($CuCl_2 \cdot 2(H_2O)$) and Pyrrole (Py) were purchased from Sigma-Aldrich. Bacterial cellulose membranes were synthesized in static culture medium according to the procedure described by Rambo et al. [19] using *Gluconacetobacter hansenii,* 558 232 ATC strain.

2.2. BNC/PPy Composite Preparation. BNC/PPy·$CuCl_2$ nanocomposites were prepared through *in situ* oxidative polymerization of Py using the copper chloride dehydrate as the oxidant agent. The hydrated BNC membranes with diameters of 30 mm were immersed in an alcoholic solution (isopropyl alcohol) with two different Py concentrations, 0.04 and 0.08 mol·L^{-1}. After 10 min under magnetic stirring, a copper chloride dehydrate alcoholic solution was added gently. The polymerization was carried out at 25°C during 4 h. After polymerization, the BNC/PPy·$CuCl_2$ membranes were washed thoroughly with acetone in order to extract the residues and byproducts of the reaction. The membranes were then vacuum dried at room temperature. The $CuCl_2 \cdot 2(H_2O)$: Py molar ratios used for the chemical synthesis were 2 : 1 and 4 : 1.

2.3. Characterization of BNC/PPy·$CuCl_2$ Composite Membranes. X-ray diffractometry was used for phase identification (XRD; Phillis, X-Pert) using Cu Kα radiation ($\lambda = 1.54$ Å). BNC/PPy·$CuCl_2$ membranes were placed on aluminum stubs and scanned over a 2θ interval between 5° and 70° with a step of 1°/min. Raman spectroscopy (InnoRam, B and WTEK) was also performed for structural analysis. The microstructure of the samples was evaluated by Field-Emission Gun Scanning Electron Microscopy (FEG-SEM, JEOL JSM-670F) operating at 15 kV and 80 A. For SEM observations, pure BNC and the BNC nanocomposites membranes were dried and placed on an aluminum support and sputtered with gold. Electrical conductivity of the BNC/PPY·$CuCl_2$ membranes was measured in ambient conditions using the four-probe method by a high precision SMU (Agilent B2912A). At least three samples of each composition were measured.

3. Results and Discussion

3.1. Chemical and Structural Analysis. The changes in the chemical structure of polypyrrole in the presence of the oxidizing agent $CuCl_2 \cdot 2(H_2O)$ as well as the oxidant agent : monomer molar ratio effect on the nanocomposites properties were studied. BNC/PPy·$CuCl_2$ composites were initially analyzed using chemical and structural analysis.

Figure 1 shows Raman spectra of BNC/PPy·$CuCl_2$ composites prepared with different Py concentrations and different oxidant agent : monomer molar ratios. Two typical peaks of polypyrrole can be observed in all samples. The typical bands of PPy are observed in the region of 1560 cm^{-1} and 1380 cm^{-1} due to the ring stretching mode and the C=C stretching of the main chain [20]. A peak is observed in the nearby region of 329 cm^{-1}, characteristic of CuO and $CuCl_2$ [21]. It can be noticed that for the composite with higher Py concentration and higher molar ratio this peak is more evident.

Figure 2 shows FTIR spectra of the bacterial cellulose nanocomposites polymerized with pyrrole using copper chloride as the oxidizing agent with different molar ratios and Py concentrations. All spectra display typical characteristics of conductive polymer as widely reported in the literature, in addition to the characteristic bands of pure $CuCl_2$ and BNC. In the $CuCl_2$ spectrum, the peaks centered at 3340 cm^{-1} and 1575 cm^{-1} correspond to the OH stretching, and the peak characteristic of Cu–Cl is located at 1129 cm^{-1} [22]. In the BNC spectrum, the 3325 cm^{-1} band is characteristic of O–H groups and the peak at 2922 cm^{-1} to asymmetric C–H bonds. The 1649 and 1028 cm^{-1} bands can be attributed to C–O and C–O–C type bonds [23]. In all other spectra, the bands observed between 1550 cm^{-1} and 1460 cm^{-1} are assigned to C–C bonds and C–N stretching vibration of the pyrrole ring, respectively. It is also observed a peak in the 1613 cm^{-1} region, corresponding to Cu^+ ion [24]. The region near the band at 1050 cm^{-1} corresponds to C–H and C–N deformation vibration. Three bands centered at around 920, 1100, and 1195 cm^{-1} correspond to the stretching vibration to the doped PPy. A band located at 1700 cm^{-1} is attributed to the carboxylic group. As can be seen, this band has been observed in many samples of polypyrrole both chemically and electrochemically polymerized. This band corresponds to the overoxidation of the C=O band of pyrrole, which influences its conductivity [25–27].

Figure 3 shows X-ray diffraction spectra of pure bacterial nanocellulose and BNC/PPy·$CuCl_2$ nanocomposites polymerized with different Py concentrations and molar ratios. For the BNC spectrum, three main diffraction peaks at 15°, 16.5°, and 22.7°, characteristic of cellulose type I, can be observed, which are attributed to the reflection planes (110), (110), and (200), respectively [28]. For the BNC/PPy·$CuCl_2$ nanocomposite with a Py concentration of 0.04 mol·L^{-1} and 4 : 1 molar ratio, characteristic peaks of copper hydroxide are observed (JCPDS 00-042-0746). The presence of copper hydroxide peaks may be related to the interaction of the BNC hydroxyl groups with the oxidizing agent. With the increase of both the Py concentration from 0.04 to 0.08 mol.L^{-1} and the molar ratio from 2 : 1 to 4 : 1, the copper hydroxide peaks are absent; however, copper chloride and traces of copper oxide peaks can be seen (JCPDS 01-072-0572). For the 2 : 1 molar ratio, peaks corresponding to the oxidizing agent are not present, only an amorphous halo, which is

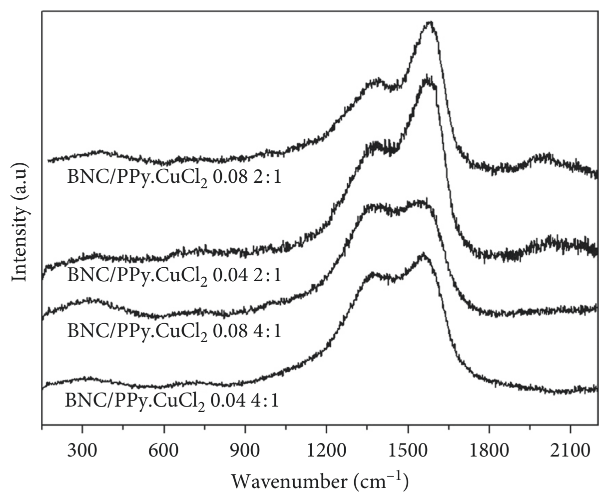

Figure 1: Raman spectra of BNC/PPy·$CuCl_2$ samples.

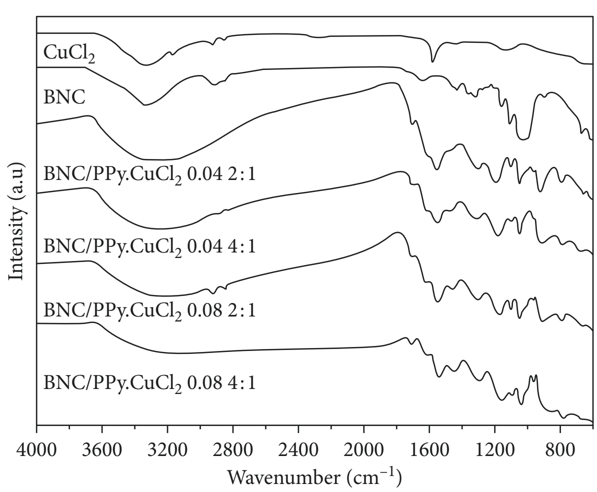

Figure 2: FT-IR spectra of BNC, $CuCl_2$, and BNC/PPy·$CuCl_2$ samples.

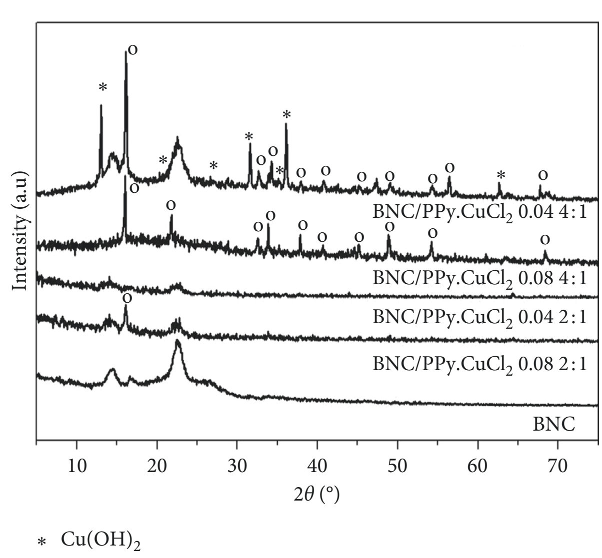

Figure 3: XRD patterns of BNC/PPy·$CuCl_2$ samples.

a characteristic of polypyrrole and the broad peaks, which are related to the bacterial cellulose.

The $CuCl_2$ present in the membranes is not chemically bound, but physically within the nanofibrous network. It is known that copper can assume valence 1 or 2, and considering that it is not chemically bound to the compound but in the form of $CuCl_2$ salt, being a simple ionic compound. The Cu valence can assume the number of oxidation +2, bivalent. Another evidence to consider this valence is the instability of the Cu^+ ions and also the low potential of Cu^{+2}/Cu^+ (0.57 V) compared to PPy (1.0 V). Because the potential is lower, receiving electrons by Cu^{+2} becomes more difficult, preventing its changing to Cu^+ [29].

3.2. Morphologic and Electrical Characterization. Figure 4 shows the morphology of the BNC/PPy·$CuCl_2$ nanocomposites polymerized with different Py concentrations and oxidizing agent : monomer molar ratios through field-emission scanning electron microscopy. BNC membranes are formed by a network structure of intertwined cellulose nanofibers with high aspect ratio [23, 30]. For the 2 : 1 molar ratio, it can be observed that at both concentrations (0.04 and 0 : 08 mol·L^{-1}), the bacterial cellulose nanofibers are coated with PPy (Figure 4(a)). As the concentration of Py increases (Figure 4(b)), an increase on the amount of PPy incorporated into the BNC matrix is observed. The increase of the concentration of Py results in an increase of the concentration of PPy particles, forming agglomerates of PPy deposited on the surface of the BNC nanofibers (Figures 4(a) and 4(b)). As the molar ratio increases from 2 : 1 to 4 : 1, an increase in the mean fiber diameter is observed, as can be also seen in Figures 4(c) and 4(d). BNC/PPy·$CuCl_2$ nanocomposites exhibited an average fiber diameter close to 300 nm; this value is four times larger than that of pure cellulose nanofibers (50 nm in average). This significant increase was not observed for 2 : 1 ratio nanocomposites, in which it was observed an average fiber diameter of 70 nm.

The electrical conductivity of the nanocomposites as a function of concentration of pyrrole and the molar ratio used in the reactions are shown in Table 1.

Pure BNC exhibits low electric conductivity, around 3.0×10^{-13} S/cm. It can be seen for the 2 : 1 molar ratio membranes that the electrical conductivity increases with the increase of PPy concentration, from 1.64×10^{-4} to 1.54×10^{-3} S/cm. For higher molar ratios, it was observed a significant increase in electrical conductivity of the nanocomposites (1.85×10^{-2} to 8.13×10^{-1} S/cm), which is two orders of magnitude higher when compared to the membrane with the same concentration and different molar ratio [9, 31]. The increase in molar ratio influenced the increase in conductivity. For higher molar ratios, the amount of copper chloride also increased, which can be the reason for higher values of electrical conductivity.

4. Conclusions

Cellulose conducting nanocomposites incorporated with polypyrrole were synthesized in a single step by in situ

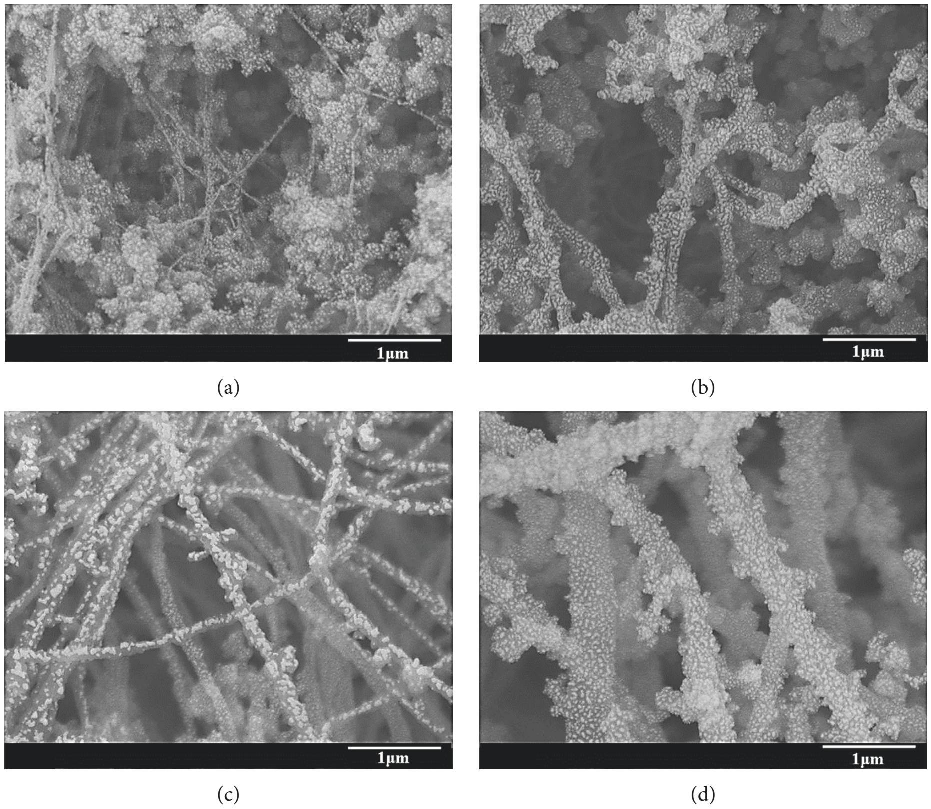

FIGURE 4: FEG-SEM micrographs of BNC/Ppy·$CuCl_2$ nanocomposites: (a) BNC/Ppy·$CuCl_2$ 0.04 2 : 1, (b) BNC/Ppy·$CuCl_2$ 0.04 4 : 1, (c) BNC/Ppy·$CuCl_2$ 0.08 2 : 1, and (d) BNC/Ppy·$CuCl_2$ 0.08 4 : 1.

TABLE 1: Electrical conductivity of BNC/PPy·$CuCl_2$ nanocomposites.

[Py] $CuCl_2 \cdot 2(H_2O)$: Py	Conductivity (S/cm)
[0.04] 2 : 1	$1.64 \times 10^{-4} \pm 1.93 \times 10^{-5}$
[0.08] 2 : 1	$1.54 \times 10^{-3} \pm 9.10 \times 10^{-3}$
[0.04] 4 : 1	$1.85 \times 10^{-2} \pm 5.94 \times 10^{-2}$
[0.08] 4 : 1	$8.13 \times 10^{-1} \pm 4.32 \times 10^{-3}$

chemical oxidative polymerization using $CuCl_2 \cdot 2(H_2O)$. The chemical and morphological characterization of the nanocomposites confirmed the presence of the conducting polymer deposited along the nanofibers and Cu-containing salts. The presence of Cu salts influenced the increase of the electrical conductivity of the nanocomposites. These nanocomposites can be promising materials in applications such as electronic devices and sensors.

Data Availability

The data used to support the findings of this study (tables and graphics) are included within the article.

Conflicts of Interest

The authors declare no conflicts of interest.

Acknowledgments

The authors gratefully thank the National Council for Scientific and Technological Development (CNPq, Brazil) and Coordination for the Improvement of Higher Level Personnel (CAPES, Brazil) for the financial support and scholarships (Grant no. 2591/2011). The authors also thank the Central Laboratory of Electronic Microscopy (LCME/UFSC).

References

[1] S. I. A. Razak, I. F. Wahab, F. Fadil, F. N. Dahli, A. Z. M. Khudzari, and H. Adeli, "A review of electrospun conductive polyaniline based nanofiber composites and blends: processing features, applications, and future directions," *Advances in Materials Science and Engineering*, vol. 2015, Article ID 356286, 19 pages, 2015.

[2] S. Kasisomayajula, N. Jadhav, and V. J. Gelling, "In situ preparation and characterization of a conductive and magnetic nanocomposite of polypyrrole and copper hydroxychloride," *RSC Advances*, vol. 6, no. 2, pp. 967–977, 2016.

[3] Q. Liu, B. Wang, J. Chen et al., "Facile synthesis of three-dimensional (3D) interconnecting polypyrrole (PPy) nanowires/nanofibrous textile composite electrode for high performance supercapacitors," *Composites Part A: Applied Science and Manufacturing*, vol. 101, pp. 30–40, 2017.

[4] J. Deng, Y. Peng, C. He, X. Long, P. Li, and A. S. Chan, "Magnetic and conducting Fe3O4-polypyrrole nanoparticles with core-shell structure," *Polymer International*, vol. 52, no. 7, pp. 1182–1187, 2003.

[5] X. Zhanga, M. Heb, P. Hea et al., "Ultrafine nano-network structured bacterial cellulose as reductant and bridging ligands to fabricate ultrathin K-birnessite type MnO_2 nanosheets for supercapacitors," *Applied Surface Science*, vol. 433, pp. 419–427, 2018.
[6] M. A. A. M. Abdah, N. A. Zubair, N. H. N. Azman, and Y. Sulaiman, "Fabrication of PEDOT coated PVA-GO nanofiber for supercapacitor," *Materials Chemistry and Physics*, vol. 192, pp. 161–169, 2017.
[7] W. Lei, L. Han, C. Xuan et al., "Nitrogen-doped carbon nanofibers derived from polypyrrole coated bacterial cellulose as high-performance electrode materials for supercapacitors and Li-ion batteries," *Electrochimica Acta*, vol. 210, pp. 130–137, 2016.
[8] Y. Liu, J. Zhou, J. Tang, and W. Tang, "Three-dimensional, chemically bonded polypyrrole/bacterial cellulose/graphene composites for high-performance supercapacitors," *Chemistry of Materials*, vol. 27, no. 20, pp. 7034–7041, 2015.
[9] D. Muller, C. R. Rambo, L. M. Porto, W. H. Schreiner, and G. M. O. Barra, "Structure and properties of polypyrrole/bacterial cellulose nanocomposites," *Carbohydrate Polymers*, vol. 94, no. 1, pp. 655–662, 2013.
[10] M. Laya, I. Gonzáleza, J. A. Tarrés, N. Pellicera, K. N. Bunb, and F. Vilaseca, "High electrical and electrochemical properties in bacterial cellulose/polypyrrole membranes," *European Polymer Journal*, vol. 91, pp. 1–9, 2017.
[11] D. Muller, J. P. Silva, C. R. Rambo, G. M. O. Barra, F. Dourado, and F. M. Gama, "Neuronal cells' behavior on polypyrrole coated bacterial nanocellulose three-dimensional (3D) scaffolds," *Journal of Biomaterials Science, Polymer Edition*, vol. 24, no. 11, pp. 1368–1377, 2013.
[12] Y. Wei, Q. Hu, Y. Cao et al., "Polypyrrole nanotube arrays on carbonized cotton textile for aqueous sodium battery," *Organic Electronics*, vol. 46, pp. 211–217, 2017.
[13] X. Li, Y. Wu, K. Hua et al., "Vertically aligned polyaniline nanowire arrays for lithium-ion battery," *Colloid and Polymer Science*, vol. 296, no. 8, pp. 1395–1400, 2018.
[14] M. Omastováa, K. Mosnáčková, M. Trchová et al., "Polypyrrole and polyaniline prepared with cerium(IV) sulfate oxidant," *Synthetic Metals*, vol. 160, no. 7-8, pp. 701–707, 2010.
[15] M. M. Ayad and M. A. Shenashin, "Polyaniline film deposition from the oxidative polymerization of aniline using $K_2Cr_2O_7$," *European Polymer Journal*, vol. 40, no. 1, pp. 197–202, 2004.
[16] G. Li, L. Jiang, and H. Peng, "One-dimensional polyaniline nanostructures with controllable surfaces and diameters using vanadic acid as the oxidant," *Macromolecules*, vol. 40, no. 22, pp. 7890–7894, 2007.
[17] J. Hur, K. Im, S. W. Kim et al., "Polypyrrole/agarose-based electronically conductive and reversibly restorable hydrogel," *ACS Nano*, vol. 8, no. 10, pp. 10066–10076, 2014.
[18] P. Lv, X. Wang, and H. Zou, "Chemical synthesis and characterization of conducting poly(2-Aminothiazole)," *Materials Science Forum*, vol. 867, pp. 111–115, 2016.
[19] C. R. Rambo, D. O. S. Recouvreux, C. A. Carminatti, A. K. Pitlovanciv, R. V. Antônio, and L. M. Porto, "Template assisted synthesis of porous nanofibrous cellulose membranes for tissue engineering," *Materials Science and Engineering: C*, vol. 28, no. 4, pp. 549–554, 2008.
[20] S. P. Lim, A. Pandikumar, Y. S. Lim, N. M. Huang, and H. N. Lim, "In-situ electrochemically deposited polypyrrole nanoparticles incorporated reduced graphene oxide as an efficient counter electrode for platinum-free dye-sensitized solar cells," *Scientific Reports-UK*, vol. 4, no. 1, 2014.
[21] A. G. M. Da Silva, T. S. Rodrigues, A. L. A. Parussulo et al., "Controlled synthesis of nanomaterials at the undergraduate laboratory: $Cu(OH)_2$ and CuO nanowires," *Journal of Chemical Education*, vol. 94, no. 6, pp. 743–750, 2017.
[22] D. G. Thakurata, A. Kalyan, R. Sen, and R. Bhattacharjee, "Vibrational IR active spectra of copper (II) chloride and cobalt (II) chloride: a combined experimental and theoretical lie algebraic study," *Journal of Computational and Theoretical Nanoscience*, vol. 11, no. 3, pp. 776–780, 2014.
[23] D. Müller, C. R. Rambo, D. O. S. Recouvreux, L. M. Porto, and G. M. O. Barra, "Chemical in situ polymerization of polypyrrole on bacterial cellulose nanofibers," *Synthetic Metals*, vol. 161, no. 1-2, pp. 106–111, 2011.
[24] A. Mohammadi, I. Lundström, O. Inganiis, and W. R. Salaneck, "Conducting polymers prepared by template polymerization: polypyrrole," *Polymer*, vol. 31, no. 3, pp. 395–399, 1990.
[25] P. Gemeinera, J. Kulicek, M. Mikula et al., "Polypyrrole-coated multi-walled carbon nanotubes for the simple preparation of counter electrodes in dye-sensitized solar cells," *Synthetic Metals*, vol. 210, pp. 323–331, 2015.
[26] W. Van Zoelen, S. Bondzic, T. F. Landaluce et al., "Nanostructured polystyrene-block-poly(4-vinyl pyridine)(pentadecylphenol) thin films as templates for polypyrrole synthesis," *Polymer*, vol. 50, no. 15, pp. 3617–3625, 2009.
[27] M. Jaymand, "Poly(4-chloromethyl styrene-g-4-vinylpyridine)/TiO_2 thin films as templates for the synthesis of polypyrrole in the nanometer-sized domain," *Designed Monomers and Polymers*, vol. 14, no. 5, pp. 433–444, 2011.
[28] C. Tokoh, K. Takabe, M. Fujita, and H. Saiki, "Cellulose synthesized by acetobacter xylinum in the presence of acetyl glucomannan," *Cellulose*, vol. 5, no. 4, pp. 249–261, 1998.
[29] X. Li, Y. Gao, X. Zhang et al., "Polyaniline/CuCl nanocomposites prepared by UV rays irradiation," *Materials Letters*, vol. 62, no. 15, pp. 2237–2240, 2008.
[30] Y. Wan, D. Hu, G. Xiong, D. Li, R. Guo, and H. Luo, "Directional fluid induced self-assembly of oriented bacterial cellulose nanofibers for potential biomimetic tissue engineering scaffolds," *Materials Chemistry and Physics*, vol. 149-150, pp. 7–11, 2015.
[31] S. Peng, L. Fan, W. Rao, Z. Bai, W. Xu, and J. Xu, "Bacterial cellulose membranes coated by polypyrrole/copper oxide as flexible supercapacitor electrodes," *Journal of Materials Science*, vol. 52, no. 4, pp. 1930–1942, 2017.